

Mechanisms of exciton energy transfer in Scheibe aggregates

J. A. Tuszynski and M. F. Jørgensen

Department of Physics, University of Alberta, Edmonton, Alberta, Canada T6G 2J1

D. Möbius

Max-Planck-Institut für Biophysikalische Chemie, Postfach 2841, D-37018 Göttingen, Germany

(Received 16 July 1997; revised manuscript received 19 October 1998)

In this paper we provide a critical reassessment of the most important physical mechanisms in Langmuir-Blodgett Scheibe aggregates. Specific issues discussed involve the hierarchy of time and energy scales, estimates of model parameters, and their consequences in terms of physical behavior. In particular, we address the issue of determining the strength of the exciton-phonon interaction and its effect on the formation and dynamics of a coherent exciton domain. [S1063-651X(99)05004-7]

PACS number(s): 61.43.Hv

I. INTRODUCTION

An extremely interesting class of Langmuir-Blodgett thin films that represent compact aggregates of dye molecules composed of chromophores and fatty acids was discovered independently in the late 1930s by Scheibe [1] in Germany and Jelly [2] in England. These designed molecular monolayers are, therefore, commonly referred to as either Scheibe or *J* aggregates. What was particularly unusual about these aggregates was the appearance of a new, very narrow absorption band of a longer wavelength than the monomer absorption band. Scheibe interpreted this as reversible polymerization effects. Subsequently, in the late 1960s and in the 1970s, it was observed by Kuhn, Möbius, and their associates [3–7] that when irradiated with uv or visible light, donor fluorescence in these monolayers was strongly quenched. Simultaneously, an acceptor fluorescence line appeared whose amplitude was almost equal to that of the primary donor spectral line, but its peak was slightly redshifted. This observation was interpreted as giving evidence that the Scheibe aggregate acts as a cooperative molecular array which, after absorbing a photon, channels the energy laterally over distances of up to 1000 Å to a particular energy-accepting molecule (an acceptor dye).

Interestingly, the efficient energy capture and transfer phenomena that characterize the Scheibe aggregates disappear with the aggregates' loss of rigidity or regular order. Somewhat paradoxically, energy capture by acceptor molecules becomes more efficient with increasing temperature. Furthermore, optimal efficiency properties are achieved for very low acceptor-to-donor concentrations. For example, at ratios on the order of $1:10^4$, over 50% of the light energy is transferred to acceptor molecules. Because of the above properties, Scheibe aggregates have sometimes been called photon energy funnels.

The importance of Scheibe aggregates lies both in fundamental and applied aspects of their functioning. Their primary application is in photographic and photodetection processes. However, potential applications in the design of solar energy cells as well as in light-operated devices such as photoresistors and photomemory have also been considered [8]. Furthermore, an understanding of the mechanism of energy

transfer in Scheibe aggregates could lead to a better microscopic theory of photon absorption in living cells.

The primary motivation for this paper is a critical reassessment of the physical mechanisms at play in the energy capture and transfer processes in Scheibe aggregates. Our objective is to use simple physical arguments in establishing the relative importance of a number of mechanisms involved. For example, extensive studies were undertaken to understand aggregates of pseudocyanine within the Frenkel exciton picture where diagonal disorder in chains with nearest-neighbor interactions was implemented [9]. Fidler and co-workers [10,11] investigated the role of both diagonal and off-diagonal disorder in the optical properties including the line shape. Models based on linear exciton interactions with nearest neighbors in the presence of shallow impurity potentials were developed [12] and simulations of thermal disorder effects indicated qualitative agreement with experiment [13]. Another group of researchers emphasized the role of nonlinearity in the efficiency of energy capture and transfer [14–18]. Finally, temperature-dependent superradiant decay and the associated dephasing-induced damping were studied in [19–22]. We wish to present estimates of energy and time scales for excitons, phonons, their mutual interactions, and the heat bath (thermal effects). Feasibility arguments will be given for various possible models of transport of the exciton energy in the monolayer. A number of these features were separately treated throughout the literature on this subject but, we believe, no single effort has been made to date in order to compare and contrast the several models which are in parallel existence.

II. THE EXCITON MODEL

A typical Scheibe aggregate structure that will be considered in the present paper is a thin film with a brick-layer arrangement of constituent dye molecules [6,7]. Two types of structurally similar molecules are being used in the aggregate: (a) an acceptor molecule (commonly thiocyanine), and (b) a donor molecule, most often oxacyanine. Their chemical structural similarity is also seen through only slight differences in their molecular weights, viz., $M_a = 1.25 \times 10^{-24}$ kg and $M_d = 1.21 \times 10^{-24}$ kg for the two cases given above,

which would indicate close resemblance of their lattice dynamics. The dimensions of the brick-layer structure are given by $a = 16 \text{ \AA}$, $b = 3.0 \text{ \AA}$, and $c = 8.0 \text{ \AA}$ [23].

As can be seen from the experimental absorption intensity profile [7], the monomer absorption line is centered at $\lambda_{\text{mono}} = 384 \text{ nm}$, which corresponds to the energy $\hbar\Omega = 3.23 \text{ eV}$. Thus, we can crudely represent the monomer as a two-level system with the second-quantized Hamiltonian of the form

$$H_{\text{mono}} = \hbar\Omega A^\dagger A. \quad (2.1)$$

On the other hand, the absorption line of the dimer is centered at $\lambda_{\text{dimer}} = 368 \text{ nm}$, corresponding to the energy of $E_{\text{dimer}} = 3.37 \text{ eV}$. Assuming that the exciton energy can be transferred between two neighboring molecules via a hopping mechanism, the simplest second-quantized Hamiltonian for the dimer has been postulated as [24]

$$H_{\text{dimer}} = (\hbar\Omega)(A_1^\dagger A_1 + A_2^\dagger A_2) - J(A_1^\dagger A_2 + A_2^\dagger A_1), \quad (2.2)$$

where J is the hopping constant and it should approximately correspond to the dipole-dipole interaction energy calculated earlier in the extended dipole model [5]. The indices 1 and 2 label the two neighboring molecules. It is easy to diagonalize the Hamiltonian matrix for the dimer and we obtain its eigenvalues as

$$E_{\text{dimer}} = \hbar\Omega \pm J. \quad (2.3)$$

We, therefore, infer that $J \approx 140 \text{ meV}$, which compares favorably with the extended dipole moment estimate we present next. Unfortunately, at this stage we are unable to deduce the sign of J and consequently predict whether the ground state is symmetric or antisymmetric. Finally, Grad, Hernandez, and Mukamel [19] used an estimate of $J \approx 75 \text{ meV}$, which is close to the range obtained in the extended dipole model [5].

In a purely excitonic model with nearest-neighbor coupling, we have the dispersion relation

$$\begin{aligned} E(\vec{k}) &= \hbar\Omega - 2 \sum_{i=1}^4 J_i \cos(\vec{k} \cdot \vec{d}_i) \\ &= \hbar\Omega - 2J_1 \cos(ak_x) - 4J_2 \cos(ak_x/2) \cos(bk_y) \\ &\quad - 2J_3 \cos(2bk_y), \end{aligned} \quad (2.4)$$

where $\vec{d}_1 = (a, 0)$, $\vec{d}_2 = (a/2, b)$, $\vec{d}_3 = (0, 2b)$, and $\vec{d}_4 = (-a/2, b)$. Here J_1 and J_3 are the horizontal and vertical coupling constants, respectively, while J_2 and J_4 are the two diagonal coupling constants. Due to symmetry we have $J_2 = J_4$. The constant term $\hbar\Omega$ is the on-site exciton energy.

Of utmost importance to our understanding of the underlying physical mechanisms is a reasonably accurate estimate of the coupling constants. This, of course, depends on the mutual orientation of the adjacent molecules. This problem has been dealt with in this context by Czikkely, Försterling, and Kuhn [4,5], who proposed an extended dipole model. With the arrangement given in Fig. 1 they calculated the interaction constant semiclassically via

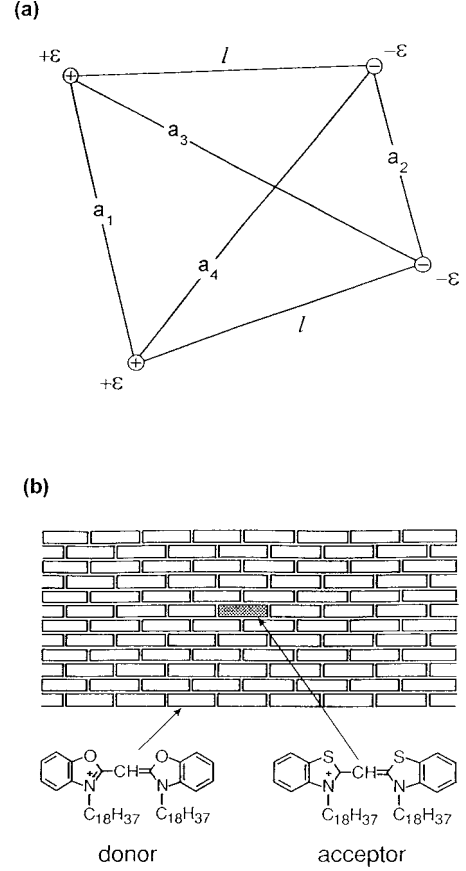


FIG. 1. An arrangement of molecules (a) and extended dipoles (b) in the extended dipole calculation.

$$J = \frac{q^2}{\epsilon} \left(\frac{1}{a_1} + \frac{1}{a_2} - \frac{1}{a_3} - \frac{1}{a_4} \right), \quad (2.5)$$

where q is an elementary charge, ϵ the dielectric constant of the medium, and the distances a_1, \dots, a_4 are explained in Fig. 1. The values of q and l were estimated to be $q = 0.22e$ and $l = 8.9 \text{ \AA}$ [4]. For $\epsilon \approx 2.5\epsilon_0$ we then find

$$J_1 = -20 \text{ meV}, \quad J_2 = -50 \text{ meV}, \quad J_3 = 52 \text{ meV}. \quad (2.6)$$

For these values the dispersion relation of Eq. (2.4) is shown in Fig. 2. At $\vec{k} = (0, 0)$ the energy surface $E(\vec{k})$ exhibits a saddle point with a negative effective mass along one axis and a positive mass along the other. It is worth noting that the possibility of a negative effective mass of a Scheibe aggregate has been recently raised by Kirstein and Mohwald [25].

The ground state (lowest energy) is located at $\vec{k} = (0, \pi/b)$ and has a value of

$$E_0 = \hbar\Omega - 2J_1 + 4J_2 - 2J_3 = \hbar\Omega - 2.65 \text{ eV}, \quad (2.7)$$

which is given relative to the on-site and deformation energies. Expanding in a power series around the ground state we obtain

$$E(\vec{k}) = E_0 + J_x a^2 k_x^2 + J_y b^2 (k_y - \pi/b)^2 + \dots, \quad (2.8)$$

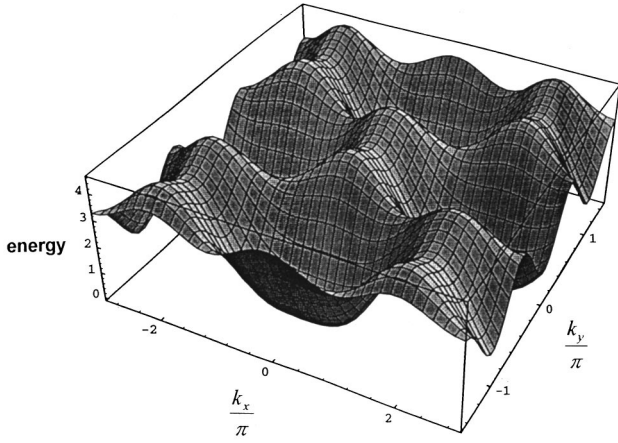


FIG. 2. Dispersion relations for the exciton energy in the Scheibe aggregate.

where the effective coupling constants J_x and J_y are given by

$$J_x = J_1 - J_2/2 = 50 \text{ meV}, \quad J_y = 4J_3 - 2J_2 = 308 \text{ meV}. \quad (2.9)$$

They are both larger than thermal energy, which at room temperature is approximately 26 meV. The effective mass components (around the equilibrium state) may now be found as

$$m_x = \frac{\hbar^2}{2a^2 J_x} = 2.8 \times 10^{-31} \text{ kg},$$

$$m_y = \frac{\hbar^2}{2b^2 J_y} = 13 \times 10^{-31} \text{ kg}. \quad (2.10)$$

In other words, the effective mass is of the same order of magnitude in both directions, which may be linked to a nearly circular and fairly isotropic domain of coherence.

III. EXCITON DOMAIN SIZE

In order to estimate the domain size of a collective exciton propagating along the molecular lattice we consider first a one-dimensional approximation of the aggregate's Hamiltonian,

$$H_{1D} = \sum_n [\hbar\Omega A_n^\dagger A_n - J A_n^\dagger (A_{n-1} + A_{n+1})], \quad (3.1)$$

where only the nearest neighbors have been included. This exciton Hamiltonian can be diagonalized by recasting it in reciprocal (momentum) variables as

$$H_{\text{ex}} = \sum_k \hbar\tilde{\Omega}(k) \tilde{A}_k^\dagger \tilde{A}_k, \quad (3.2)$$

where the dispersion formula is in one dimension and including only the nearest neighbors gives

$$\tilde{\Omega}(k) = D - 2J \cos k \quad (3.3)$$

while the creators and annihilators are

$$\tilde{A}_k^\dagger = \frac{1}{\sqrt{2\pi}} \sum_n e^{-ikn} A_n^\dagger \quad (3.4)$$

and

$$\tilde{A}_k = \frac{1}{\sqrt{2\pi}} \sum_n e^{+ikn} A_n. \quad (3.5)$$

This formulation immediately indicates the presence of only two characteristic parameters: the hopping constant J and the lattice spacing d which defines the maximum momentum (edge of the Brillouin zone): $k_0 = \pi/d$. For example, it follows that the characteristic energy for collective excitons is on the order of

$$E_{\text{ex}} = 2J \approx 0.3 \text{ eV} \quad (3.6)$$

and the characteristic temperature is

$$T_{\text{ex}} = \frac{2J}{k_B} \approx 3.5 \times 10^3 \text{ K}. \quad (3.7)$$

In the continuum approximation the energy dispersion is of the form

$$E(k) = Jd^2 k^2, \quad (3.8)$$

where d is the lattice spacing. The two-site correlation function is defined as

$$\Gamma(\xi) = \int_{-\infty}^{\infty} A^\dagger(x) A(x + \xi) dx, \quad (3.9)$$

where $A(x)$ and $A^\dagger(x)$ are the annihilation and creation operators in the site representation. In the Fourier (momentum) representation we replace $A(x)$ with $a(k)$ and the corresponding expression is

$$\Gamma(\xi) = \int_{-\infty}^{\infty} a^\dagger(k) a(k) e^{-ik\xi} dk, \quad (3.10)$$

the mean occupation number of the k th mode is

$$\langle a^\dagger(k) a(k) \rangle = K \exp\left[-\frac{E(k)}{k_B T}\right], \quad (3.11)$$

and the normalization constant K is found to be

$$K = d \left(\frac{J}{\pi k_B T} \right)^{1/2}. \quad (3.12)$$

We insert these equations into the correlation function, which in turn evaluates to

$$\Gamma(\xi) = \exp\left[-\frac{\xi^2}{2\xi_{\text{cor}}^2}\right], \quad (3.13)$$

with

$$\xi_{\text{cor}} = d \left(\frac{2J}{k_B T} \right)^{1/2}. \quad (3.14)$$

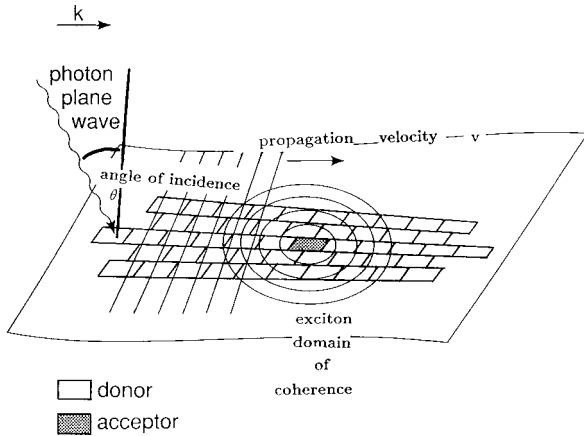


FIG. 3. An illustration of the process of the creation of a coherent exciton domain by a photon; following [43].

Thus the two-site correlation function is Gaussian and we interpret the width ξ_{cor} as the correlation length (or the size of the coherent domain).

The two-dimensional analog, domain size A , is then approximately given by the product of the correlation length in the x and y directions, i.e.,

$$A = 2ab \frac{\sqrt{J_x J_y}}{k_B T} \approx 9.5ab. \quad (3.15)$$

This result shows that the exciton size is inversely proportional to the absolute temperature, in agreement with the analysis by Möbius and Kuhn [23], and at room temperature covers approximately 10 lattice sites. This latter finding is very important since it can be linked with an empirical relationship derived by Möbius and Kuhn, who noted that the size of the domain of coherence is [23]

$$N_{\text{eff}} = \frac{3000}{[T(\text{K})]}. \quad (3.16)$$

Approximating N_{eff} at 300 K gives us the above formula almost exactly. The correlation length may be expressed in terms of effective mass m_{eff} as

$$\xi_{\text{cor}} = \frac{\hbar}{\sqrt{m_{\text{eff}} k_B T}}. \quad (3.17)$$

As mentioned earlier, since the effective mass is anisotropic, it follows that the exciton domain is oval-shaped.

It is of considerable interest to know the magnitude of m_{eff} . Depending on the direction of propagation and the actual value of J taken, we expect m_{eff} to range between $0.9 \times 9 \times 10^{-31}$ and 3×10^{-30} kg, i.e., it is expected to be very small. For subsequent estimates we assume that $10^{-31} \leq m_{\text{eff}} \leq 10^{-30}$ kg.

We shall now discuss the process of launching an exciton domain by a photon as shown in Fig. 3. The first estimate we make in this context is the maximum initial velocity of the exciton domain. This occurs for $\Theta \approx 90^\circ$, where Θ is the angle of incidence measured with respect to the normal to the film, and a completely inelastic scattering (absorption) of

electromagnetic radiation. Then $p_\lambda = p_{\text{ex}}$, which means that the maximum velocity of the exciton is

$$v_0^{\text{max}} = \frac{p_\lambda}{m_{\text{eff}}} = \frac{h}{\lambda_p m_{\text{eff}}} \approx 1 \times 10^4 \text{ m/s}, \quad (3.18)$$

for $\lambda = 366 \text{ nm}$ [23]. This is very interesting since it is of the same order of magnitude (but lower) as the average propagation velocity of an exciton inferred from the experiments of Möbius and Kuhn [23]. As a consequence, the exciton in all likelihood is accelerated, probably by the presence of impurity acceptors. The second estimate concerns the size of the coherent exciton domain. The Heisenberg uncertainty principle $\Delta x \Delta p \geq \hbar$ should give us an idea of the minimal spatial extent of the domain. Since $\Delta p(0) \approx \hbar \omega / c$ we easily find that $\Delta x(0) \geq 500 \text{ \AA}$, which corresponds to approximately 120 lattice spacings along the brick width and 30 lattice spacings along its length.

Furthermore, based on Gaussian wave packet spreading phenomena, one expects this domain of coherence to grow in size over time. The question we wish to pose is, how large will the domain become when the center reaches an acceptor molecule? Taking the acceptor-to-donor ratio of $1:10^4$ leads to an average distance of 100 lattice spacings or approximately 10^{-7} m . Following Möbius and Kuhn [23] we take the average speed of exciton propagation of $v_{\text{ex}} = 2 \times 10^4 \text{ m/s}$, which gives the flight time of $\tau_{\text{flight}} = 5 \text{ ps}$. A long-time approximation for the Gaussian wave packet spreading can be taken as

$$\Delta x(\tau) \approx \frac{\hbar}{\Delta x(0) m_{\text{eff}}} \tau. \quad (3.19)$$

This expression assumes the coupling with lattice vibrations to be negligible. Substituting the numbers discussed above gives $\Delta x(\tau_{\text{flight}}) \approx 10^{-7} \text{ m}$, i.e., the size of the domain has doubled in each direction and it now covers an area approximately equal to the entire space available between neighboring acceptors. What we are tempted to conclude from this simple calculation is that a mechanism is needed to focus this energy and transfer it eventually to a well-localized acceptor site. One possible way of causing localization is through an inclusion of nonlinear effects. Another eventuality is related to the presence of impurity sites as shallow energy potentials leading to a binding process. Both cases have been studied in the past and we briefly summarize the latter mechanism below.

Bartnik, Blinowska, and Tuszyński [24] have suggested that the acceptor eigenenergy lies slightly below that of the donor (approximately 10%). Simultaneously they assumed the acceptor hopping constant to be 10–20% lower than that of the donor. In their simulations a one-dimensional rigid exciton lattice was adopted and the results indicated the possibility of efficient energy transfer to acceptor sites at optimal parameter values. Subsequent simulations included an additive white noise in the coupling constant J that was intended to mimic the role of thermal disorder in the Scheibe lattice. Encouragingly, increasing the noise level to a value corresponding to the standard deviation of approximately 1.5% resulted in an improved capture efficiency. A further increase in the noise level caused an eventual destruction of

the exciton energy transfer to an acceptor site. This would indicate that shallow energy levels of acceptor molecules may indeed cause the observed effects. A discussion concerning the role of nonlinearity in the formation and maintenance of a coherent domain will be given in a later section. It is worth mentioning here, however, that the nonlinear effects of exciton localization may indeed be related to impurity trapping and have been investigated in other contexts including fluorescence of photosynthetic systems on spectrally disordered lattices [26,27].

IV. RANDOM WALK MODEL

Having established a basis for the existence of a *domain of coherence* we now turn to the question of its motion towards an acceptor molecule. The first input into this discussion comes from an estimate of the kinetic energy of the center-of-mass motion of an exciton domain. We find that

$$E_{\text{kin}} \approx \frac{1}{2} m_{\text{eff}} v_{\text{ex}}^2 \approx 0.1 \text{ meV}, \quad (4.1)$$

assuming after Möbius and Kuhn [23] that $v_{\text{ex}} \approx 2 \times 10^4$ m/s. This is an exceedingly small amount of energy. For example, thermal energy (for two degrees of freedom) ranges from approximately 3 to 30 meV for temperatures between 30 and 300 K, respectively. Hence, unless there is significant effective friction opposing the domain's motion, it will execute random motion similar to a quasifree gas molecule. However, this line of thinking poses further problems. While an estimate of rms velocity of such motion is very high, namely,

$$v_{\text{rms}} = \sqrt{2k_B T / m_{\text{eff}}}, \quad (4.2)$$

which ranges between 4×10^4 and 2×10^5 m/s for $T = 30$ and 300 K, respectively, its interpretation puts this picture in question. If the random walk process is unbiased, the domain's most probable position is still the original starting point, i.e., as far from the acceptor molecule as in the beginning. In order to arrive at a feasible mechanism we suggest a biased random walk picture instead. This would imply the probability of a step towards the closest acceptor site given by q and away from it by p ($q > p$). Of course, the same argument would apply to both directions and motion in the two perpendicular directions would be statistically independent.

We assume that the exciton moves about on a brick-layered lattice as outlined earlier. Each site has eight nearest neighbors as shown in Fig. 4. The exciton domain is assumed to be circular with the center located at one of the sites and a radius r . The radius is assumed to be independent of time and, for the present purpose, we neglect any initial velocity due to momentum transfer from the photon. Furthermore, it is assumed that the exciton momentum during the random walk process is negligible compared to the momentum transfer from interactions with the lattice phonons. This relies on the assumption of large damping and will likely be true at large temperatures.

We then introduce the position vectors $\vec{l}_1, \dots, \vec{l}_8$ corresponding to the eight nearest neighbors given by

$$\vec{l}_1 = (a, 0),$$

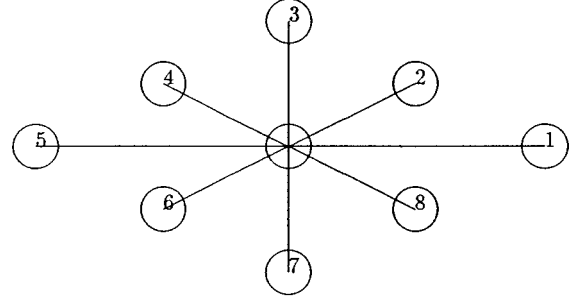


FIG. 4. The eight nearest neighbors of each site.

$$\vec{l}_2 = (a/2, b),$$

$$\vec{l}_3 = (0, 2b),$$

$$\vec{l}_4 = (-a/2, b),$$

and $\vec{l}_5 = -\vec{l}_1$, $\vec{l}_6 = -\vec{l}_2$, $\vec{l}_7 = -\vec{l}_3$, and $\vec{l}_8 = -\vec{l}_4$. Here a and b are the length and width of each brick. The exciton performs a biased random walk across this lattice. Hence, at each time step τ the motion is characterized by eight transition probabilities, p_1, \dots, p_8 . The probability p_0 of remaining at the same site is then determined by the normalization condition $p_0 + \dots + p_8 = 1$. The acceptors may either be distributed randomly across the lattice or placed in a regular superlattice. Each acceptor gives rise to a potential energy $U_n(r)$, which we assume to be of Coulomb type,

$$U_n(r) = U_0 \frac{l}{r_n}. \quad (4.3)$$

Here, U_0 is the difference in eigenenergy between donor and acceptor sites, l is an average lattice spacing, and r_n is the distance to the acceptor labeled n . The exciton thus experiences a total potential energy given by

$$U = U_0 \sum_n \frac{l}{r_n}. \quad (4.4)$$

The transition probabilities p_i depend only on two variables: the energy difference ΔU_i and the hopping constant J_i . They must be proportional to the latter and we assume an exponential dependence of the probability on the energy difference during the step, i.e.,

$$\frac{p_i}{p_0} = \alpha J_i \exp[-\beta \Delta U_i], \quad (4.5)$$

where α and β are two yet undetermined parameters. To approximate the energy difference we assume that the potential energy varies slowly across the lattice, and we therefore obtain

$$\Delta U_i \approx \vec{\nabla} U \cdot \vec{l}_i, \quad (4.6)$$

where

$$\vec{\nabla}U = U_0 l \sum_n \frac{\vec{r}_n}{r_n^3}. \quad (4.7)$$

Inserting these expressions into Eq. (4.5) gives

$$\frac{p_i}{p_0} = \alpha J_i \exp[-\gamma \vec{f} \cdot \vec{l}_i], \quad (4.8)$$

where $\gamma = \beta U_0 l$ and

$$\vec{f} = \sum_n \frac{\vec{r}_n}{r_n^3}. \quad (4.9)$$

Implementing this procedure, one then finds a net drift towards a more probable acceptor given by

$$\langle x \rangle = N(q-p)d, \quad (4.10)$$

where N is the number of steps, i.e., $N = t/\tau_0$ with τ_0 denoting the average hopping time of approximately $\tau_0 = 3 \times 10^{-14}$ s [6]. Incidentally, the above estimate of τ_0 corresponds almost exactly to the fluorescence bandwidth of 8–9 nm observed in these compact host lattice assemblies [6,23]. Thus, the average propagation velocity is given by

$$u_{\text{ex}} = \frac{\langle x \rangle}{t} = \frac{d}{\tau} (q-p), \quad (4.11)$$

which, with $d_{\perp} = 3 \text{ \AA}$, $d_{\parallel} = 16 \text{ \AA}$, and $\tau_0 = 3 \times 10^{-14}$ s, indicates a need for a very strong bias along the width of the brick-layer structure in order to reach speeds exceeding 10^4 m/s (i.e., $q \approx 1$ and $p \approx 0$). In the opposite case, propagating along the long axis would require a reduction by a factor of 2, which translates into $q = \frac{3}{4}$ and $p = \frac{1}{4}$, so that the net velocity would be 2×10^4 m/s as argued in [23] on a different basis.

The biased random walk framework brings us closer to another possible point of view, namely, a unidirectional motion towards an acceptor, which could be caused by the attractive presence of a shallow energy level at the acceptor site. Since we established earlier on that the initial exciton velocity cannot exceed 1×10^4 m/s (average propagation speed), this means that the motion should be accelerated by a force. Taking the depth of the acceptor level as $\Delta E \approx 0.3$ eV and assuming that it is removed by 100 lattice sites from the center of the coherence domain yields an average force \bar{F} of between 0.02 and 0.08 pN. Assuming further that the domain starts from rest we arrive at an estimate of the average propagation velocity as

$$\bar{v} \approx \left(\frac{\bar{F} \Delta l}{2m_{\text{eff}}} \right)^{1/2} \approx 5 \times 10^5 \text{ m/s}, \quad (4.12)$$

which is off by an order of magnitude. However, this force will be distributed inhomogeneously and friction will slow the motion down.

We conclude that far away from an impurity site, a small domain (i.e., at high temperatures) is likely to execute a random walk with a bias that becomes more pronounced close to an acceptor site. However, high concentrations of acceptor sites and low temperature ranges are likely to lead to a be-

havior that is far more unidirectional and far less random. Furthermore, radiative losses are expected to be greater at low temperatures, since the domain size is larger.

V. PHONONS

An important aspect that so far has been ignored in our discussion is the effect of lattice vibrations on both the formation of a coherent exciton domain (giving it lifetime) and on its propagation (providing effective friction). Following standard texts on solid state theory [28], the Hamiltonian for the lattice phonons can be written as

$$H_{\text{ph}} = \int \hbar \omega_k (b_k^\dagger b_k + \frac{1}{2}) dk, \quad (5.1)$$

where the dispersion relation in ω_k depends on the type of phonons considered (optical or acoustic, etc.) and b_k^\dagger , b_k are the phonon creation and annihilation operators, respectively.

Inoue [8] fitted the tail of the absorption spectrum for merocyanine using the Urbach rule [29] and obtained an estimate of the effective phonon energy as $\hbar \omega = 30.3$ meV. Spano, Kuklinski, and Mukamel [20] obtained a similar value of $\hbar \omega = 29.8$ meV for optical phonons in pseudocyanine. The above estimates show that the phonon energy is roughly an order of magnitude smaller than the average exciton hopping energy and two orders of magnitude smaller than the on-site exciton energy, i.e., we infer that

$$\frac{\hbar \omega}{J} \approx 0.2, \quad \frac{\hbar \omega}{\hbar \Omega} \approx 10^{-2}. \quad (5.2)$$

The characteristic phonon temperature (the Debye temperature) is

$$T_{\text{ph}} = \frac{\hbar \omega}{k_B} \approx 350 \text{ K} \quad (5.3)$$

and the characteristic phonon time scale is

$$\tau_{\text{ph}} \approx \frac{1}{\omega} \approx 2 \times 10^{-14} \text{ s}, \quad (5.4)$$

which is very close to the hopping time τ_0 , indicating a strong possibility of coupling between these two types of excitations. The on-site lattice fluctuations are found to be

$$u_{\text{rms}} \approx (0.1 \text{ \AA}) \times \left(\frac{T}{T_{\text{ph}}} \right)^{1/2}, \quad (5.5)$$

which is consistent with an analogous discussion presented in [13].

The phonon velocity depends both on the type of phonon and on the direction of propagation. For acoustic phonons we find

$$v_{\text{ph}} = \frac{\hbar \omega}{\hbar (\pi/d)} \approx (0.6-2.5) \times 10^4 \text{ m/s}, \quad (5.6)$$

which is quite comparable to the average exciton velocity, indicating a strong possibility of coupling between these two types of excitations. Finally, the effective phonon mass is

$$m_{\text{ph}} \simeq \frac{\hbar \tau_{\text{ph}}}{d^2} \simeq 10^{-29} - 10^{-30} \text{ kg} \quad (5.7)$$

depending on the direction of propagation, i.e., one to two orders of magnitude greater than the effective exciton mass.

VI. EXCITON-PHONON COUPLING

The root cause of exciton-phonon coupling is the distance dependence of the excitonic parameters Ω and J . As a consequence, the simplest way an interaction energy of this type can be written is

$$H_{\text{int}} = \chi_1 \sum_n (u_{n+1} - u_{n-1}) A_n^\dagger A_n + \chi_2 \sum_n (u_{n+1} - u_n) \times (A_{n+1}^\dagger A_n + A_n^\dagger A_{n+1}). \quad (6.1)$$

It has recently been shown [30] that these two coupling terms (proportional to χ_1 and χ_2) tend to inhibit each other and their combined effect may be conveniently represented by the single dimensionless parameter

$$\alpha = \frac{\chi_1 - \chi_2}{2J\sqrt{Mk_B T_{\text{ph}}}}. \quad (6.2)$$

A preliminary estimate of the magnitudes of χ_1 and χ_2 indicates that $\chi_1 \approx 100$ pN [31] and $\chi_2 \approx J/(3d) \approx 40$ pN. It will be useful to convert these values into energy units so we define

$$\chi_{\text{eff}} = (\chi_1 - \chi_2)d, \quad (6.3)$$

and obtain an estimate of χ_{eff} as 16–60 meV depending on the direction.

Inoue [8] concluded that the exciton-phonon coupling applies to a two-dimensional case and inferred from the experiments for merocyanine that its strength is approximately given by $\chi_{\text{eff}} \approx 29$ meV. Spano, Kuklinski, and Mukamel [20] estimated $\chi_{\text{eff}} \approx 26$ meV, which is quite consistent with it.

The total Hamiltonian for the aggregate can, therefore, be written as

$$\begin{aligned} H &= H_{\text{ex}} + H_{\text{ph}} + H_{\text{ex-ph}} \\ &= \sum_n [\hbar\Omega A_n^\dagger A_n - J(A_n^\dagger A_{n+1} + A_{n+1}^\dagger A_n)] \\ &\quad + \sum_n \left[\frac{p_n^2}{2M} + \frac{1}{2} K(u_n - u_{n+1})^2 \right] \\ &\quad + \chi_1 \sum_n [A_n^\dagger A_n (u_{n+1} - u_{n-1})] \\ &\quad + \chi_2 \sum_n [(A_n^\dagger A_{n+1} + A_{n+1}^\dagger A_n)(u_{n+1} - u_n)], \end{aligned} \quad (6.4)$$

which can be compactly recast into its momentum representation as

$$\begin{aligned} H &= \sum_k [\hbar\Omega_k a_k^\dagger a_k + \hbar\omega_k (b_k^\dagger b_k + \frac{1}{2})] \\ &\quad + \sum_{k,l} \chi_{\text{eff}}(k) (b_k^\dagger + b_{-k}) a_{k+l}^\dagger a_l. \end{aligned} \quad (6.5)$$

The dynamics of the combined system is determined by just two parameters: α , which was introduced earlier, and $\beta = T_{\text{ex}}/T_{\text{ph}}$ [30]. Depending on the values of α and β one finds four possible regimes: (a) $\alpha < 1$ and $\beta < 1$, (b) $\alpha < 1$ and $\beta > 1$, (c) $\alpha > 1$ and $\beta < 1$, and (d) $\alpha > 1$ and $\beta > 1$. It appears that we are dealing here with $\beta \gg 1$ and $\alpha \ll 1$, which leads to the breakdown of the adiabatic approximation. The maximum velocity of localized excitonic soliton wave packets is bounded by the sound velocity. This causes a coherence dephasing of the exciton whose rate is proportional to J [30].

Furthermore, the significant presence of exciton-phonon coupling introduces nonlinearity into the problem. There exist two standard approaches to treat this difficulty: (a) for weak nonlinearities adopt a perturbative scheme, which can be done fully quantum mechanically, and (b) for sufficiently strong nonlinearities the above method fails and one solves the problem semiclassically by incorporating nonlinear terms in the classical equations of motion in the continuum limit. Below, we discuss the importance of nonlinearity in the dynamics of Scheibe aggregates.

VII. THE ROLE OF NONLINEARITY

The equations of motion for the displacement variable u_n and the exciton amplitude A_n can be readily found from the full exciton-phonon Hamiltonian as

$$\begin{aligned} M\ddot{u}_n &= k(u_{n+1} - 2u_n + u_{n-1}) + \chi_1 (A_{n+1}^\dagger A_{n+1} - A_{n-1}^\dagger A_{n-1}) \\ &\quad - \chi_2 (A_n^\dagger A_{n-1} + A_{n-1}^\dagger A_n - A_{n+1}^\dagger A_n - A_n^\dagger A_{n+1}) \end{aligned} \quad (7.1)$$

and

$$\begin{aligned} i\hbar\dot{A}_n &= [\hbar\Omega + \chi_1(u_{n+1} - u_{n-1})]A_n \\ &\quad + [J + \chi_2(u_{n+1} - u_n)]A_{n+1} \\ &\quad + [J + \chi_2(u_n - u_{n-1})]A_{n-1}. \end{aligned} \quad (7.2)$$

The continuum limit consists of two approximations. First, the Taylor expansions for the two variables are truncated at the second order terms, i.e.,

$$u_{n\pm 1} \simeq u(x) \pm d \frac{\partial u}{\partial x} + \frac{d^2}{2} \frac{\partial^2 u}{\partial x^2} + \dots \quad (7.3)$$

and

$$A_{n\pm 1} \simeq d^{1/2} \left(A(x) \pm d \frac{\partial A}{\partial x} + \frac{d^2}{2} \frac{\partial^2 A}{\partial x^2} + \dots \right). \quad (7.4)$$

Second, the sums over n appearing in the Hamiltonian are replaced with integrals according to

$$\sum_n \simeq \frac{1}{d} \int dx. \quad (7.5)$$

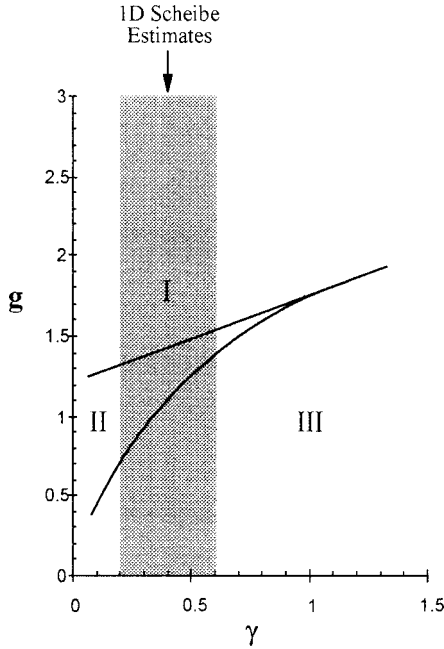


FIG. 5. The three regimes of behavior for one-dimensional exciton-phonon systems; following [32].

As a result, the following coupled equations of motion are found in the continuum limit:

$$\frac{\partial^2 u}{\partial t^2} - v_0^2 \frac{\partial^2 u}{\partial x^2} = \frac{2d}{\rho} (\chi_1 - \chi_2) \frac{\partial}{\partial x} |A|^2 + \frac{d^3}{\rho} \left[\frac{(\chi_1 - \chi_2)}{18} \frac{\partial^3 (|A|^2)}{\partial x^3} + \chi_2 \frac{\partial}{\partial x} \left(\left| \frac{\partial A}{\partial x} \right|^2 \right) \right] \quad (7.6)$$

and

$$i\hbar \frac{\partial A}{\partial t} = \left((\hbar\Omega - 2J) + 2d(\chi_1 - \chi_2) \frac{\partial u}{\partial x} \right) A - d^2 \hbar J \frac{\partial^2 A}{\partial x^2} + d^3 \left[\frac{(\chi_1 - \chi_2)}{3} \frac{\partial^3 u}{\partial x^3} A - \chi_2 \frac{\partial}{\partial x} \left(\frac{\partial u}{\partial x} \frac{\partial A}{\partial x} \right) \right], \quad (7.7)$$

where $\rho = M/d$ is the linear mass density, $|A|^2 = A^\dagger A$ implies a classical approximation, and the third order terms are usually ignored.

A recent paper [32] discussed three possible regimes of behavior in the one-dimensional approach to the exciton-phonon coupled systems described above. Depending on the values of the two parameters $\gamma = \hbar\omega_{\text{ph}}/J$ and $g = |\chi|^2/(2\hbar\omega_{\text{ph}}J)$, the three regimes found correspond to (a) delocalized, almost free exciton (region I), (b) the small polaron limit (region III), and (c) the self-trapped exciton state (region II). Figure 5 demonstrates the location of these regimes on the parameter plane.

Admittedly, the Scheibe aggregate is a two-dimensional system and a straightforward application of these results may be misleading. Nevertheless, we have evaluated the range of parameters g and γ based on the estimates arrived at earlier, i.e.,

$$\hbar\omega_{\text{ph}} \approx 30 \text{ meV}, \quad (7.8)$$

$$50 \text{ meV} \leq J \leq 150 \text{ meV}, \quad (7.9)$$

$$25 \text{ meV} \leq \chi_{\text{eff}} \leq 100 \text{ meV}. \quad (7.10)$$

This results in $0.2 \leq \gamma \leq 0.6$ and $0.07 \leq g \leq 3.3$, which is still inconclusive but the largest area covered favors either a free exciton or a small polaron picture, at least in the quasi-one-dimensional picture. This is somewhat reassuring in light of what was argued earlier in the paper. The rather large size of the domain of coherence and a relatively weak exciton-phonon coupling emphasized in our paper are suggestive of a nearly free exciton drifting to an impurity site under thermal noise with a possible role of nonlinearity in preventing the wave packet from spreading.

There have been a number of studies that focused on the role of nonlinearity in more realistic two-dimensional models (but still in the continuum approximation). One such nonlinear model was proposed by Huth, Gutmann, and Vitiello [14]. The model was derived by treating the phonons classically and subsequently eliminating them via an adiabatic approximation which, in view of this paper's findings, is not entirely justified. In the continuum limit, Huth, Gutmann, and Vitiello [14] derived a two-dimensional cubic nonlinear Schrödinger equation [33–35], where the energy transfer takes place through solitonlike ring waves. The dynamics is described by collapsing ring waves and the collapse time was associated with the effective exciton lifetime [15,16]. Bang and co-workers [17,18] further showed that the effect of temperature is to increase the collapse time and decrease the coherence time, which seems to be in contradiction with experimental data [21,36–39]. More recent investigations [40,41,31] involving the formation and propagation of nonlinear localized coherent structures in two dimensions included the presence of Gaussian impurity potentials due to acceptor molecules. Their results are much better correlated with experimental observations. However, what appears to be needed in a future study of nonlinear effects in two-dimensional lattices is the introduction of a negative effective mass along one of the two directions of propagation, which might be how an exciton domain is originally created. It appears that in a hyperbolic version of the two-dimensional nonlinear Schrödinger equation (which would correspond to such a scenario), the effect of a negative signature in the two-dimensional Laplacian is to increase the stability of a solitary wave, which takes the form of a bright soliton along one direction and a dark soliton along the other direction [42]. Recently, Christiansen *et al.* [43] initiated such a study for a 2D nonlinear Schrödinger model with dispersive dipole-dipole interactions but encountered cumbersome instabilities of the solutions.

One effect that has not yet been discussed in the present work is the role of radiative losses. It is believed that an exciton domain of coherence radiates its energy at a rate that is proportional to its size, i.e.,

$$k_{\text{rad}} = N_{\text{eff}} \text{ ns}^{-1}. \quad (7.11)$$

Mukamel and his collaborators [19,20] proposed a model to incorporate radiative losses via the incorporation of an imaginary term in the exciton-phonon Hamiltonian. As a re-

sult, these authors found that the effective size of a coherent exciton domain, N_{eff} , is proportional to this imaginary part of the exciton-phonon Hamiltonian and hence increasing the absolute temperature T causes the size of the domain, N_{eff} , to decrease in proportion to T . This, in turn, decreases the radiative decay, causing an elongation of the lifetime, in agreement with experimental results.

VIII. CONCLUSIONS

In this paper we have been concerned with a number of physical mechanisms that are at play in the processes of energy capture and transfer in Scheibe aggregates. It was argued based on fundamental principles of quantum mechanics that the photon energy harvested by a monolayer must necessarily be highly delocalized when it is initially absorbed by donor molecules. The thus created domain of exciton coherence is then subjected to a number of influences. The main effects can be summarized as follows: (a) quantum decoherence due to wave packet spreading—this may possibly be arrested by nonlinearity, (b) thermalization which affects the size of the domain—the exciton coupling with phonons appears to conform to the semiempirical formula $N_{\text{eff}} = (3000 \text{ K})/T$, and (c) the attractive influence of acceptor molecules [44]. The latter effect is perhaps the least studied and merits careful examination.

We may, therefore, conclude that there exist several competing processes with their own time scales and it is imperative to determine which of these processes are dominant under the conditions of various impurity concentrations. We will attempt a summary by including the following processes.

- (a) Unidirectional propagation of a domain of coherence: It is governed by center-of-mass motion and its characteristic time scale is given by the time of flight

$$\tau_{\text{flight}} = \frac{\Delta l}{v_{\text{ex}}}, \quad (8.1)$$

where Δl is the mean donor-to-acceptor distance and v_{ex} will be assumed on the order of 2×10^4 m/s.

- (b) Radiative decay: Its characteristic time scale is given by the size of the domain of coherence and we adopt the formula [23,20]

$$\tau_{\text{rad}} \approx (1 \text{ ns}) \frac{T}{3000 \text{ K}}. \quad (8.2)$$

- (c) Exciton-phonon interactions: assuming a weak coupling, and hence the absence of soliton formation, leads to the lifetime formula of an exciton given by [40]

$$\tau_{\text{ex-ph}} = \frac{2\hbar J}{\chi^2(2\bar{n} + 1)}, \quad (8.3)$$

where

$$\bar{n} = \frac{1}{\exp(T_{\text{ph}}/T) - 1} \quad (8.4)$$

is the mean occupation number for phonons. It is also well known that $\tau_{\text{ex-ph}}$ is inversely proportional to the width of an absorption line.

TABLE I. A summary of characteristic time estimates.

N_d/N_a	T (K)	τ_{flight} (s)	τ_{rad} (s)	$\tau_{\text{ex-ph}}$ (s)	τ_{diff} (s)
10^2	30	10^{-12}	10^{-11}	10^{-13}	0.6×10^{-11}
10^2	300	2×10^{-12}	10^{-10}	5×10^{-14}	4×10^{-11}
10^4	30	10^{-10}	10^{-11}	10^{-13}	4×10^{-8}
10^4	300	2×10^{-10}	10^{-10}	5×10^{-14}	4×10^{-7}

- (d) Diffusion processes: For high concentrations of acceptors and high temperature ranges, diffusive propagation of an exciton domain may compete with the above processes. The characteristic time scale is determined by the mean diffusion time

$$\tau_{\text{diff}} = \frac{(\Delta l)^2}{D}, \quad (8.5)$$

where $D = v_{\text{ex}}^2 \tau_{\text{ex-ph}}$.

In Table I we have summarized the results of our rough estimates for the four different time scales at two temperatures $T = 30$ and 300 K as well as two concentration values $N_d:N_a = 10^2$ and 10^4 . The idea is to find out which mechanisms dominate the picture in each of the four regimes of control parameter values (high/low temperature and high/low acceptor concentrations).

Based on Table I the following can be concluded. First, exciton-phonon interactions lead to a rapid thermalization process of the exciton domain. Depending on the strength of the coupling we then deal with a ‘‘dressed-up’’ collective exciton structure. Phonons are not expected to determine the capture process at an acceptor site. Second, diffusive propagation of the exciton domain is very unlikely to play a major role, except possibly at very high concentrations of acceptor molecules. Depending on the actual parameter values, either radiative losses or the speed of unidirectional propagation towards an acceptor will determine the fate of an exciton domain. It would now appear that at low acceptor concentrations the most important effect is the radiative loss process, which limits the probability of exciton energy capture. However, at high acceptor concentrations exciton propagation velocity is sufficiently high to reach an acceptor molecule before any excessive energy loss has occurred [45].

In summary, we wish to emphasize that the processes of exciton energy capture and transfer via Scheibe aggregates may be more complex and multifaceted than any hitherto proposed model has emulated. Work on a fuller two-dimensional description of the processes is underway.

ACKNOWLEDGMENTS

Y. Gaididei and P. L. Christiansen are acknowledged for many fruitful and inspiring discussions. J.A.T. wishes to thank NSERC (Canada) for support and the Institute of Mathematical Modelling at the Technical University of Denmark for partial support and hospitality during his visit to Lyngby. M.F.J. expresses gratitude for support from NATO and the Danish Technical Research Council under Grant No. STVF/9600179.

- [1] G. Scheibe, *Angew. Chem.* **49**, 567 (1936).
- [2] E. E. Jelly, *Nature (London)* **138**, 1009 (1936).
- [3] V. Czikkely, G. Dreizler, H. D. Försterling, H. Kuhn, J. Sondermann, P. Tillmann, and J. Wiegand, *Z. Naturforsch. A* **24A**, 1823 (1969).
- [4] V. Czikkely, H. D. Försterling, and H. Kuhn, *Chem. Phys. Lett.* **6**, 11 (1970).
- [5] V. Czikkely, H. D. Försterling, and H. Kuhn, *Chem. Phys. Lett.* **6**, 207 (1970).
- [6] H. Kuhn, *J. Photochem.* **10**, 111 (1979).
- [7] D. Möbius, *Ber. Bunsenges. Phys. Chem.* **82**, 848 (1978).
- [8] T. Inoue, *Thin Solid Films* **132**, 21 (1985).
- [9] E. W. Knapp, *Chem. Phys.* **85**, 73 (1984).
- [10] H. Fidder and D. A. Wiersma, *Phys. Rev. Lett.* **66**, 1501 (1991).
- [11] H. Fidder, J. Knoester, and D. A. Wiersma, *J. Chem. Phys.* **95**, 7880 (1991).
- [12] E. A. Bartnik and K. J. Blinowska, *Phys. Lett. A* **134**, 448 (1989).
- [13] E. A. Bartnik, K. J. Blinowska, and J. A. Tuszynski, *Phys. Lett. A* **169**, 46 (1992).
- [14] G. C. Huth, F. Gutmann, and G. Vitiello, *Phys. Lett. A* **140**, 339 (1989).
- [15] P. L. Christiansen, S. Pagano, and G. Vitiello, *Phys. Lett. A* **154**, 381 (1991).
- [16] P. L. Christiansen, O. Bang, S. Pagano, and G. Vitiello, *Nanobiology* **1**, 229 (1992).
- [17] O. Bang, Ph.D. thesis, The Technical University of Denmark, Lyngby, Denmark, 1993.
- [18] O. Bang, P. L. Christiansen, K. Ø. Rasmussen, and Y. B. Gaididei, in *Proceedings of the Workshop on Nonlinear Excitations in Biomolecules*, Les Houches, 1994, edited by M. Peyrard (Springer-Verlag, Berlin, 1995).
- [19] J. Grad, G. Hernandez, and S. Mukamel, *Phys. Rev. A* **37**, 3835 (1987).
- [20] F. C. Spano, J. R. Kuklinski, and S. Mukamel, *Phys. Rev. Lett.* **65**, 211 (1990).
- [21] S. DeBoer and D. A. Wiersma, *Chem. Phys. Lett.* **165**, 45 (1990).
- [22] F. C. Spano and S. Mukamel, *J. Chem. Phys.* **91**, 683 (1989).
- [23] D. Möbius and H. Kuhn, *J. Appl. Phys.* **64**, 5138 (1988).
- [24] E. A. Bartnik, K. J. Blinowska, and J. A. Tuszynski, *Nanobiology* **1**, 239 (1992).
- [25] S. Kirstein and H. Möhwald, *Adv. Mater.* **7**, 460 (1995).
- [26] R. M. Pearlstein, *Photochem. Photobiol.* **35**, 835 (1982).
- [27] J. M. J. Jean, C-K. Chan, G. R. Fleming, and T. G. Owens, *Biophys. J.* **56**, 1203 (1989).
- [28] H. Haken, *Quantum Field Theory* (North-Holland, Amsterdam, 1976).
- [29] F. Moser and F. Urbach, *Phys. Rev.* **102**, 1519 (1956).
- [30] M. F. Jørgensen, J. A. Tuszynski, and D. Sept, *Phys. Lett. A* **225**, 134 (1997).
- [31] Yu. B. Gaididei, K. Ø. Rasmussen, and P. L. Christiansen, *Phys. Rev. E* **52**, 2951 (1995).
- [32] L. S. Brizhik, A. A. Eremko, and A. La Magna, *Phys. Lett. A* **200**, 213 (1995).
- [33] V. E. Zakharov and A. B. Shabat, *Zh. Eksp. Teor. Fiz.* **61**, 118 (1971) [*Sov. Phys. JETP* **34**, 62 (1972)].
- [34] J. Juul Rasmussen and K. Rypdal, *Phys. Scr.* **33**, 481 (1986).
- [35] K. Rypdal and J. Juul Rasmussen, *Phys. Scr.* **33**, 498 (1986).
- [36] D. Möbius and H. Kuhn, *Isr. J. Chem.* **18**, 375 (1979).
- [37] H. P. Dorn and A. Müller, *Appl. Phys. B: Photophys. Laser Chem.* **43**, 167 (1987).
- [38] T. Hoh, T. Ikehara, and Y. Iwabuchi, *J. Lumin.* **45**, 29 (1990).
- [39] J. Feldman, G. Peter, E. O. Göbel, P. Dawson, K. Moore, C. Foxon, and R. J. Elliott, *Phys. Rev. Lett.* **59**, 2337 (1987).
- [40] Yu. B. Gaididei and A. A. Serikov, *Theor. Math. Phys.* **27**, 242 (1976).
- [41] Yu. B. Gaididei, K. Ø. Rasmussen, and P. L. Christiansen, *Phys. Lett. A* **203**, 175 (1995).
- [42] P. L. Christiansen (private communication).
- [43] P. L. Christiansen, Yu. B. Gaididei, M. Johansson, K. Ø. Rasmussen, V. K. Mezentsev, and J. J. Rasmussen, *Phys. Rev. B* **57**, 11 303 (1998).
- [44] E. A. Bartnik and J. A. Tuszynski, *Phys. Rev. E* **48**, 1516 (1993).
- [45] L. J. Bernstein, *Nanobiology* **1**, 251 (1992).